Supplementary Material for

Assessing the Effectiveness of SO_2, NOx, and NH_3 Emission Reductions in Mitigating Winter $PM_{2.5}$ in Taiwan Using CMAQ Model

by

Ping-Chieh Huang[1], Hui-Ming Hung[1*], Hsin-Chih Lai[2], and Charles C.-K. Chou[3]

Contents of this file

Relationship between S_{NOx,NO_3} and NO_2 concentration

The reduction in NOx emissions induces a decrease in NO_2 concentration, leading to a subsequent reduction in HNO_3 production through reaction R1.

$$\mathrm{NO_2} + \mathrm{OH} \rightarrow \mathrm{HNO_3} \quad \text{(R1)}$$

The production rate of HNO_3 (P_{HNO3}) can be calculated with OH concentration assumed in the steady state as follows:

$$\frac{\mathrm{d[OH]}}{\mathrm{dt}} = P_r - L = P - \sum k_i[A]_i\,[\mathrm{OH}] - k_{NO_2}[\mathrm{NO_2}][\mathrm{OH}], \quad (1)$$

where P_r and L are chemical production and loss of [OH], $\sum k_i[A]_i$ [OH] is the sum of reaction rates of all OH-consuming chemical reactions except (R1), k_i is the rate constant of each reaction.

The steady-state [OH] is estimated as follows:

$$[\mathrm{OH}]_{\mathrm{SS}} = \frac{P_r}{\sum k_i[A]_i + k_{NO_2}[\mathrm{NO_2}]} \quad (2)$$

$$\mathrm{P_{HNO_3}} = k_{NO_2}[\mathrm{NO_2}][\mathrm{OH}]_{\mathrm{SS}} = \frac{P_r \times k_{NO_2}[\mathrm{NO_2}]}{\sum k_i[A]_i + k_{NO_2}[\mathrm{NO_2}]} \quad (3)$$

The total [HNO_3] is contributed by the chemical process ($[\mathrm{HNO_3}]_{\mathrm{chem}}$) at a time frame of Δt and transported from outside the domain boundaries ($[\mathrm{HNO_3}]_{\mathrm{trans}}$) as follows:

$$[\mathrm{HNO_3}] = [\mathrm{HNO_3}]_{\mathrm{chem}} + [\mathrm{HNO_3}]_{\mathrm{trans}} = \frac{P_r \times k_{NO_2}[\mathrm{NO_2}]\Delta\mathrm{t}}{\sum k_i[A]_i + k_{NO_2}[\mathrm{NO_2}]} + [\mathrm{HNO_3}]_{\mathrm{trans}} \quad (4)$$

As [NO_2] low enough, $[\mathrm{HNO_3}]_{\mathrm{trans}}$ would become comparable with $[\mathrm{HNO_3}]_{\mathrm{chem}}$ to affect the total [HNO_3]. With the simple assumption of [NO_2] proportional to the emission reduction rate, i.e., [NO_2] = $[NO_2]_{control\_run}$ × *Er*, where *Er* is the emission ratio. With the assumption of P_r × Δt = 3 and $\sum k_i[A]_i : k_{NO_2}[\mathrm{NO_2}]_{\mathrm{control\_run}}$ = 7 : 5, (the assumed variable values are applied to evaluate the influence of transport term on the sensitivity, S_{NOx,NO_3}). Figure S11 shows HNO_3 concentration and S_{NOx,NO_3} in this condition with $[\mathrm{HNO_3}]_{\mathrm{trans}}$ = 0, 0.2, and 0.53, which represents no transported HNO_3, transported HNO_3 equal to $[\mathrm{HNO_3}]_{\mathrm{chem}}$ at NO_2 = 0.1 and at NO_2 = 0.3. HNO_3 increases as *Er* increases, but the increase gradually slows down. The variation in transported HNO_3 does not alter the overall pattern of total HNO_3; it only introduces differences in values (Fig. S11a). However, the trend of S_{NOx,NO_3} is different (Fig. S11b). In the absence of transported HNO_3, S_{NOx,NO_3} increases as *Er* decreases. Conversely, when $[\mathrm{HNO_3}]_{\mathrm{trans}}$ is greater than 0, S_{NOx,NO_3} has a transition point, occurring at *Er,* corresponding to a $[\mathrm{HNO_3}]_{\mathrm{chem}}$ similar to $[\mathrm{HNO_3}]_{\mathrm{trans}}$. The scatter plot of S_{NOx,NO_3} is calculated based on the six discrete points with an interval of 0.2 to mimic the CMAQ simulation and shows a similar trend under the influence of non-zero $[HNO_3]_{trans}$.

Table S1: WRF-CMAQ model setting.

	Parameters	Setting
WRF v3.7.1	Microphysics	WSM 5-class scheme
	Cumulus Parameterization	Kain-Fritsch
	Planetary Boundary Layer	YSU scheme
	Surface Layer	MM5 Monin-Obukhov scheme
	Land Surface	Unified Noah land-surface model
	Urban Surface	No
	Longwave Radiation	cam scheme
	Shortwave Radiation	cam scheme
	SST_update	Yes
CMAQ v5.2.1	Chemical mechanism	Cb06
	Horizontal advection	Yamo
	Vertical advection	WRF input
	Horizontal mixing/diffusion	Multiscale
	Aerosol	Aero 6
	Cloud option	ACM AE6
	Emission	TEDS 9.0

Table S2: WRF-CMAQ resolution.

		D01	D02	D03	D04
WRF	**Vertical Layer**	45	45	45	45
	Grid size	91×91	166×169	223×223	223×223
	FDDA	Yes	Yes	Yes	No
CMAQ	**Resolution**	81km	27km	9km	3km
	Vertical Layer	6	15	15	15
	Grid size	70×80	70×80	70×80	90×135

Table S3: Box model initial conditions.

parameter	value	Description*
Temperature	291 K	
Cloud water	0.376 g kg^{-1}	
$CO_{2(g)}$	400 ppmv	Constant
$SO_{2(g)}$	7.13 ppbv	[b]$SO_{2(g)}$ + [c]dH_2O_2
[a]$H_2O_{2(g)}$	0.43 ppbv	
[b]$O_{3(g)}$	18.7 ppbv	
Total [a]NH_3	73.4 ppbv × [d]*Er*	$NH_{3(g)}$ + NH_4^+(I+J+K)
Total [a]HNO_3	12.3 ppbv	$HNO_{3(g)}$ + NO_3^-(I+J+K)
SO_4^{2-}	0.088 μg m^{-3}	[b]SO_4^{2-}(I+J+K) – [c]dH_2O_2
[a]Fe^{3+}	0.0238 μg m^{-3}	Fe(III) available for sulfate oxidation
[a]Mn^{2+}	0.035 μg m^{-3}	Mn(II) available for sulfate oxidation
[a]Na^+	0.48	I+J+K
[a]K^+	0.82	J+K
[a]Ca^{2+}	1.38	J+K
[a]Mg^{2+}	1.00	J+K
[a]Cl^-	0.64	I+J+K

[*] I, J, K denotes Aitken, accumulation, and coarse modes in particle phase from CMAQ output.

[*] Condition: a grid point along the coast of Taichung (24.203° N, 120.5053° E, the second layer, ~ 68.5 m a.s.l) at 8:00 am local time on 3rd December 2018 from CMAQ.

[a] The concentration from the control run.

[b] The concentration from the NH3_02x run (NH_3 emission reduced to 0.2x of control run).

[c] dH_2O_2 is the H_2O_2 difference concentration (control run – NH3-02x run).

[d] *Er* ranges from 0.2 to 1.0 at 0.1 intervals

Table S4: Reactions and rate constants used in box model (from Seinfeld and Pandis (2006))

Dissolution reaction		**Henry's constant (M atm$^{=1}$)**
1.	$CO_2 + H_2O \leftrightarrow CO_2 \cdot H_2O$	$H_{CO_2} = 0.034$
2.	$SO_2 + H_2O \leftrightarrow SO_2 \cdot H_2O$	$H_{SO_2} = 1.23$
3.	$HNO_{3(g)} \leftrightarrow HNO_{3(aq)}$	$H_{HNO_3} = 2.1 \times 10^5$
4.	$NH_3 + H_2O \leftrightarrow NH_3 \cdot H_2O$	$H_{NH_3} = 62$
5.	$O_{3(g)} \leftrightarrow O_{3(aq)}$	$H_{O_3} = 1.14 \times 10^{-2}$
6.	$H_2O_{2(g)} \leftrightarrow H_2O_{2(aq)}$	$H_{H_2O_2} = 1 \times 10^5$
Dissociation reaction		**Rate constant (M)**
7.	$CO_2 \cdot H_2O \leftrightarrow HCO_3^- + H^+$ $HCO_3^- \leftrightarrow CO_3^{2-} + H^+$	$k_{c1} = 4.2 \times 10^{-7}$ $k_{c2} = 5.61 \times 10^{-11}$
8.	$SO_2 \cdot H_2O \leftrightarrow HSO_3^- + H^+$ $HSO_3^- \leftrightarrow SO_3^{2-} + H^+$	$k_{s1} = 1.3 \times 10^{-2}$ $k_{s2} = 6.6 \times 10^{-8}$
9.	$HNO_{3(aq)} \leftrightarrow NO_3^- + H^+$	$k_{a1} = 15.4$
10.	$NH_3 \cdot H_2O \leftrightarrow NH_4^+ + OH^-$	$k_{a1} = 1.7 \times 10^{-5}$
11.	$H_2SO4 \leftrightarrow HSO_4^- + H^+$ $HSO_4^- \leftrightarrow SO_4^{2-} + H^+$	as a complete dissociation $k_{a2} = 1.2 \times 10^{-2}$
12.	$H_2O \leftrightarrow H^+ + OH^-$	
Aqueous oxidation reaction		**Rate constant (M^{-1}s^{-1})**
13.	$SO_2 + O_3 + H_2O \rightarrow SO_4^{2-} + O_2 + 2H^+$ $HSO_3^- + O_3 \rightarrow SO_4^{2-} + O_2 + H^+$ $SO_3^{2-} + O_3 \rightarrow SO_4^{2-} + O_2$	$k_{O_3,1} = 2.4 \times 10^4$ $k_{O_3,2} = 3.7 \times 10^5$ $k_{O_3,2} = 1.5 \times 10^9$
14.	$HSO_3^- + H_2O_2 + H^+ \rightarrow SO_4^{2-} + 2H^+ + H_2O$	$k_{H_2O_2} = 7.45 \times 10^7$
15.	$S(IV) + \frac{1}{2}O_2 \xrightarrow{Mn^{2+},Fe^{3+}} S(VI)$	$k_{Mn} = 750; k_{Fe} = 2600;$ $k_{Mn,Fe} = 1.0 \times 10^{10}$

Table S5: Statistic of air temperature, relative humidity, CO, and O_3 of MOENV observation and model simulation.

	Tamsui	Shalu	Taixi	Qianzhen
Temperature (degree C)				
Mean value of MOENV	18.61	20.19	20.00	23.31
Mean value of WRF	18.48	19.50	19.05	22.39
Correlation coefficient	0.87	0.93	0.84	0.93
Mean bias error	-0.18	-0.69	-0.95	-0.92
Mean absolute error	1.33	1.10	1.47	1.34
RH (%)				
Mean value of MOENV	85.12	74.97	82.85	69.49
Mean value of WRF	80.42	76.49	80.71	69.95
Correlation coefficient	0.71	0.84	0.58	0.86
Mean bias error	-4.23	1.52	-2.14	0.46
Mean absolute error	7.31	6.23	6.75	4.78
CO (ppbv)				
Mean value of MOENV	331.98	355.42	258.98	644.20
Mean value of CMAQ	137.84	143.09	129.03	266.13
Correlation coefficient	0.59	0.53	0.46	0.62
Mean bias error	-194.05	-212.32	-129.94	-377.72
Mean absolute error	196.13	212.32	130.95	378.77
O_3 (ppbv)				
Mean value of MOENV	35.05	31.43	37.74	26.77
Mean value of CMAQ	47.13	42.73	42.57	32.51
Correlation coefficient	0.66	0.73	0.58	0.84
Mean bias error	12.07	11.29	4.67	5.76
Mean absolute error	13.0	12.93	8.94	11.05

$$\text{Correlation coefficient} = \frac{\sum_{i=1}^{n}(m_i-\bar{m})(o_i-\bar{o})}{\sqrt{\sum_{i=1}^{n}(m_i-\bar{m})^2}\sqrt{\sum_{i=1}^{n}(o_i-\bar{o})^2}}$$

Mean bias error $= \overline{(m_i - o_i)}$; Mean absolute error $= \overline{|(m_i - o_i)|}$

where m_i and o_i are the wind speed or concentrations of model and observation at time i, respectively, and $\overline{m}$ and $\bar{o}$ are their average over December 2018.

Table S6: Mean contribution of sulfate formation in each air pollution zone (altitude below 200m a.s.l.).

	Gas phase processes	Aqueous phase processes	Other processes
northern Taiwan	8.4 %	21.5 %	70.1 %
Chu-Miao area	11.2 %	28.5 %	60.3 %
central Taiwan	13.2 %	30.5 %	56.3 %
Yun-Chia-Nan area	16.5 %	27.6 %	55.9 %
Kao-Ping area	19.8 %	23.7 %	56.6 %

Table S7: Statistics of $PM_{2.5}$ sensitivity coefficient of NOx ($S_{NOx,PM_{2.5}}$) and NH_3 ($S_{NH_3,PM_{2.5}}$) in each air pollution zone (altitude below 200m a.s.l.) under the current condition (at NOx emission ratio of 0.9).

	$S_{NOx,PM_{2.5}}$			$S_{NH_3,PM_{2.5}}$		
	Mean	**Q1**	**Q3**	**Mean**	**Q1**	**Q3**
Northern Taiwan	0.15	0.12	0.19	0.12	0.11	0.14
Chu-Miao area	0.20	0.18	0.22	0.17	0.16	0.19
Central Taiwan	0.23	0.20	0.25	0.19	0.18	0.21
Yun-Chia-Nan area	0.33	0.30	0.36	0.19	0.18	0.20
Kao-Ping area	0.34	0.31	0.41	0.19	0.17	0.21

Mean: Arithmetic mean; Q1: 25th percentile; Q3: 75th percentile.

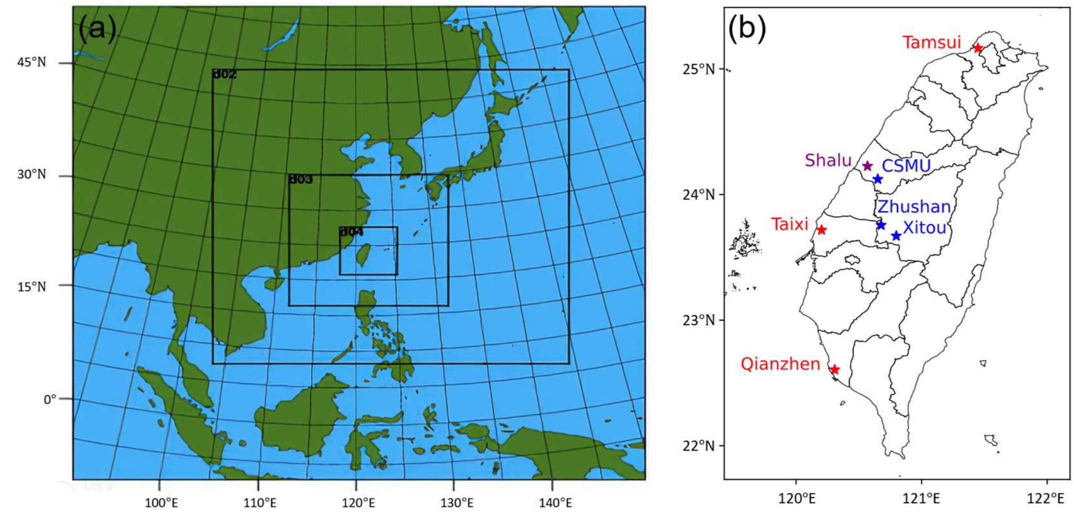

Figure S1: (a) WPS domain configuration. (b) CMAQ d04 domain. Red points are MOENV stations. Blue points are PM components measurement stations. Purple point is Shalu station, having both EPA data and PM components data.

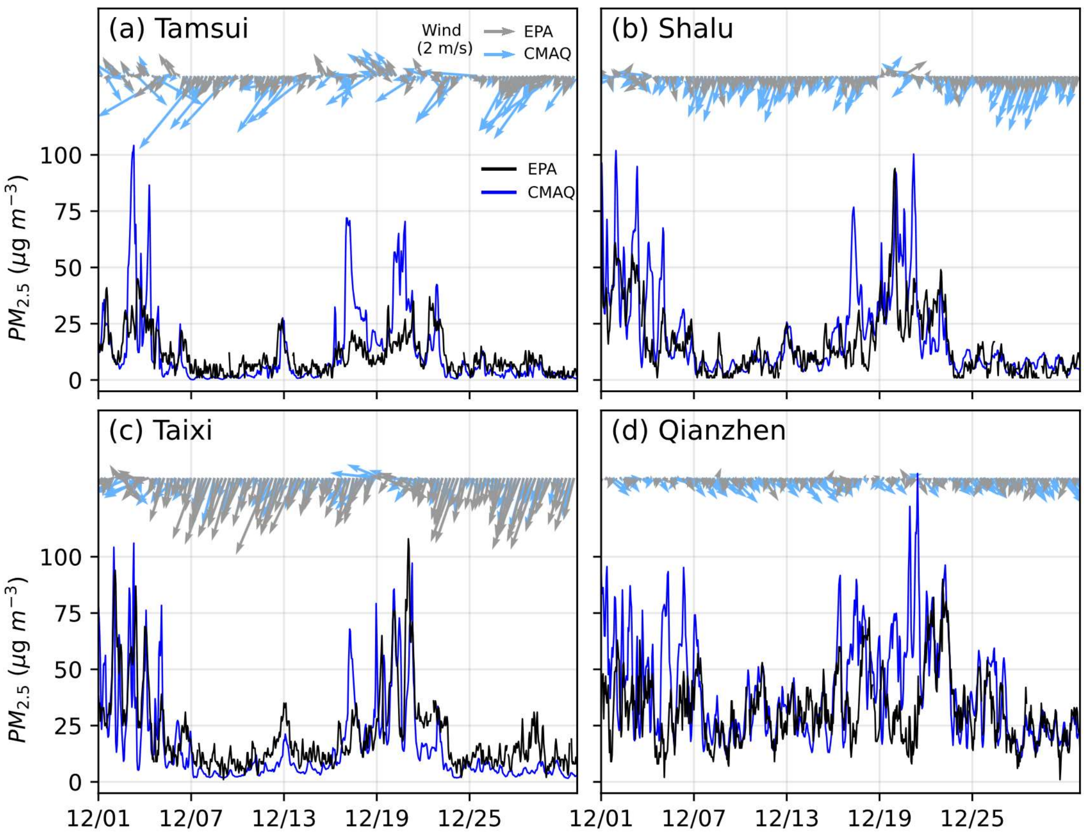

Figure S2: The comparison of wind field and $PM_{2.5}$ between MOENV ground observation and CMAQ surface layer.

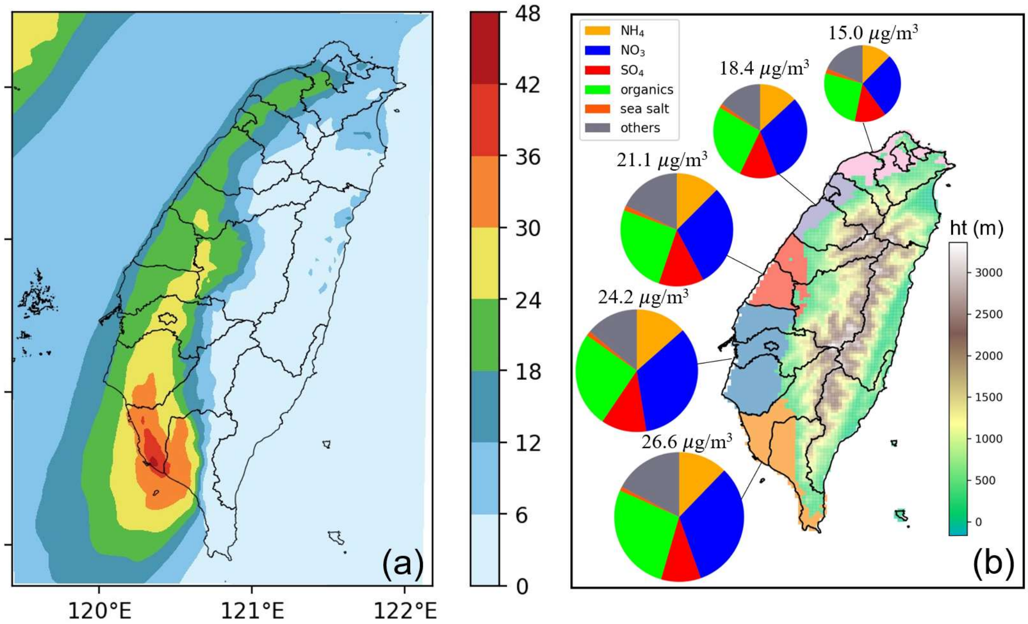

Figure S3: (a) Average $PM_{2.5}$ concentration (μg m^{-3}). (b) The composition fraction and $PM_{2.5}$ concentrations for different regions (different shading colors) at less than 200 m altitude above sea level. (From north to south, the regions are northern Taiwan (pink), Chu-Miao (purple), central Taiwan (red), Yun-Chia-Nan (blue), and Kao-Ping (orange)). The component is shown in legend. The colorbar is the height above sea level. Conditions: average data from 1-31 December 2018 for the surface layer.

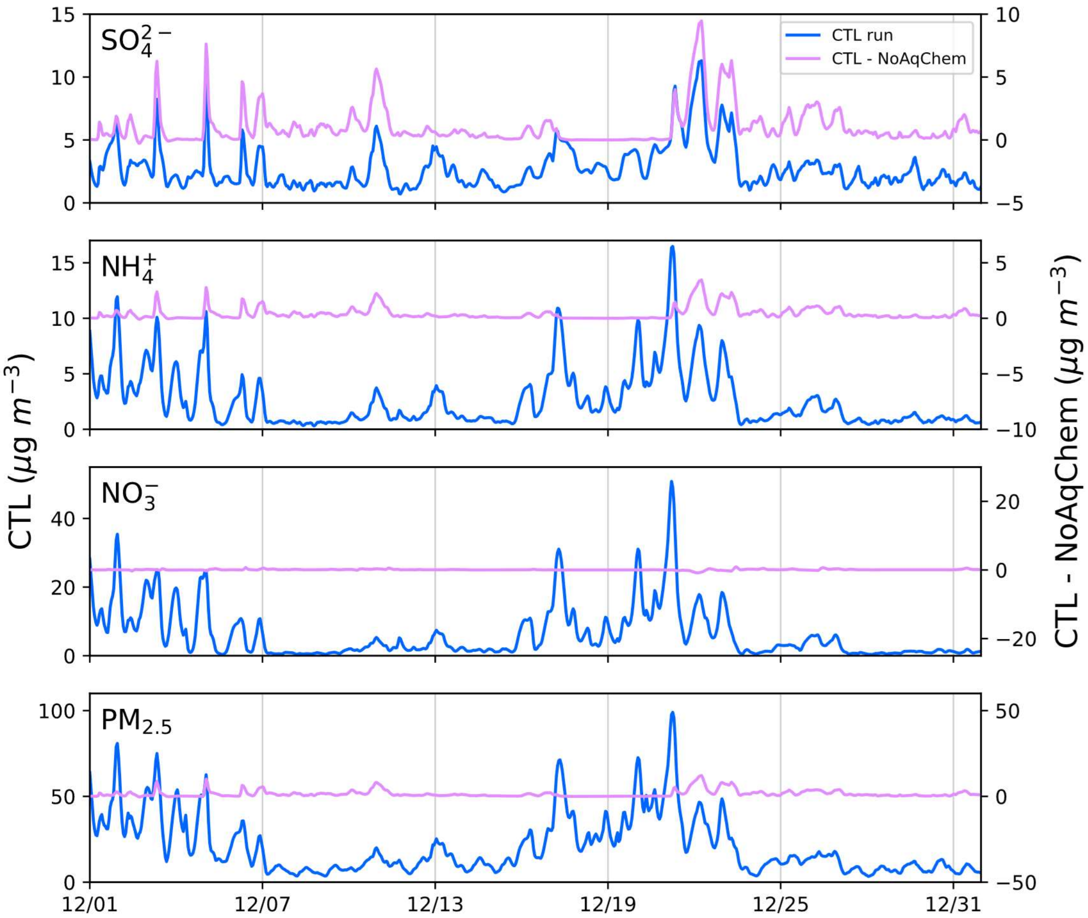

Figure S4: Sulfate, ammonium, nitrate, and $PM_{2.5}$ concentrations of control run (blue line, left y-axis) and difference between control and NoAqChem run (pink line, right y-axis). The left and right y-axes have the same scale but different ranges. Conditions: average data of central Taiwan for the surface layer.

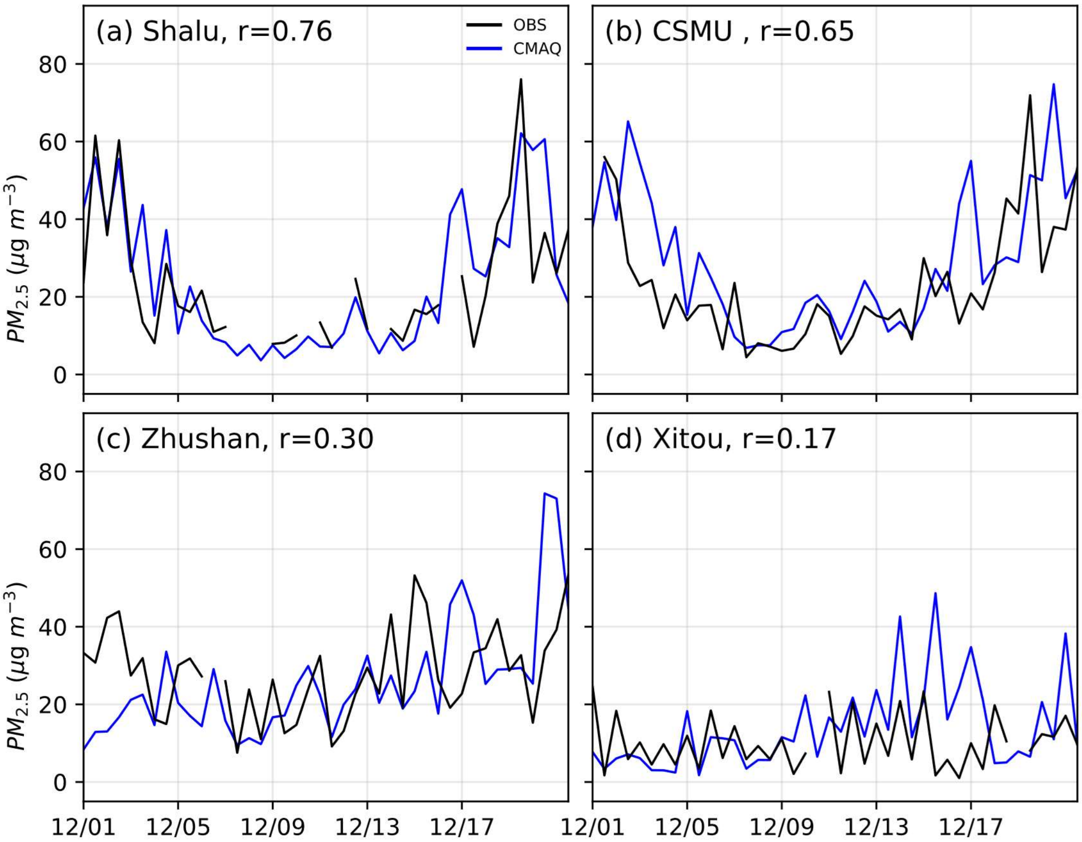

Figure S5: The comparison of $PM_{2.5}$ between observation and CMAQ surface layer in central Taiwan (r: correlation coefficient).

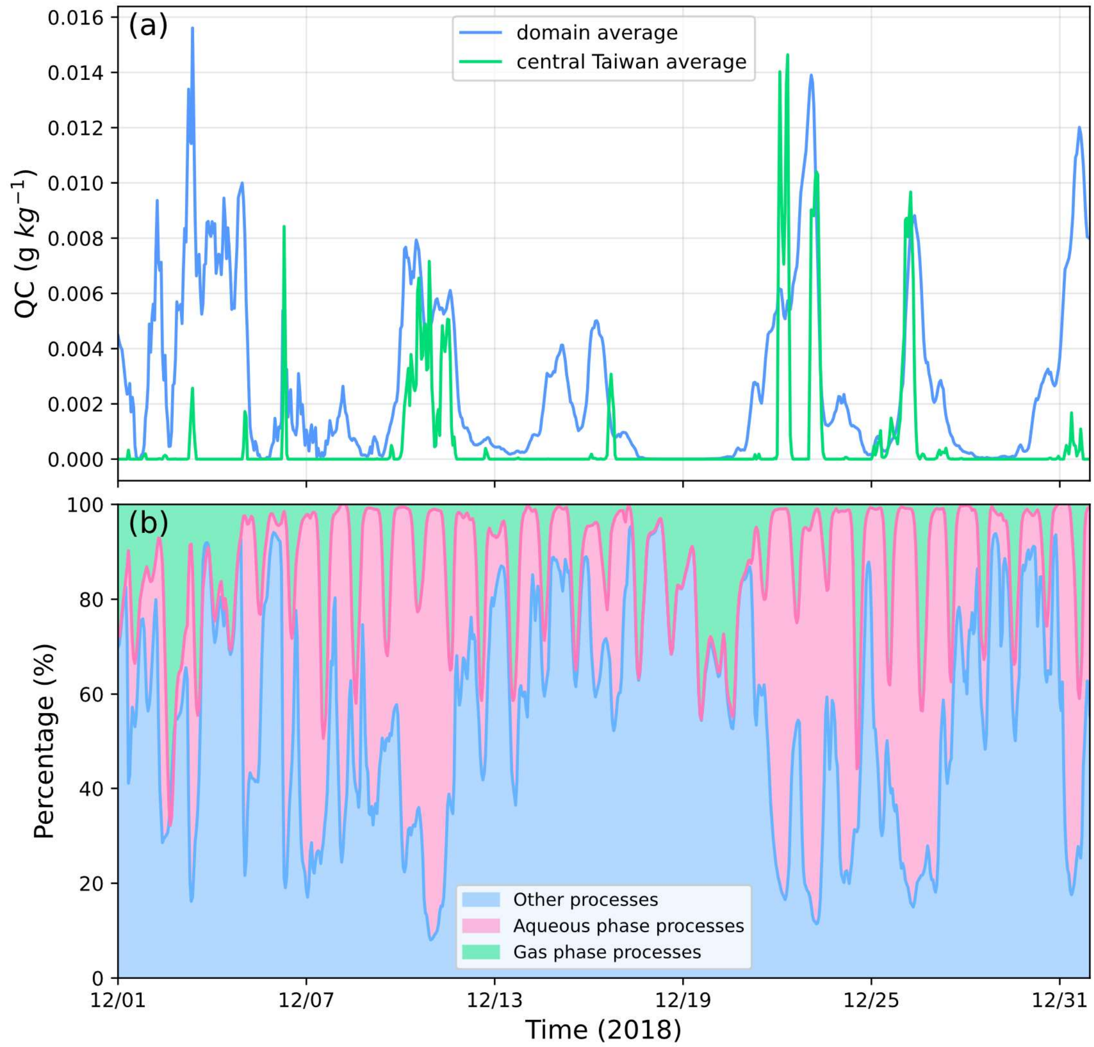

105

Figure S6: (a) Average cloud water within the planetary boundary layers. (b) Surface layer average sulfate source contributions in central Taiwan.

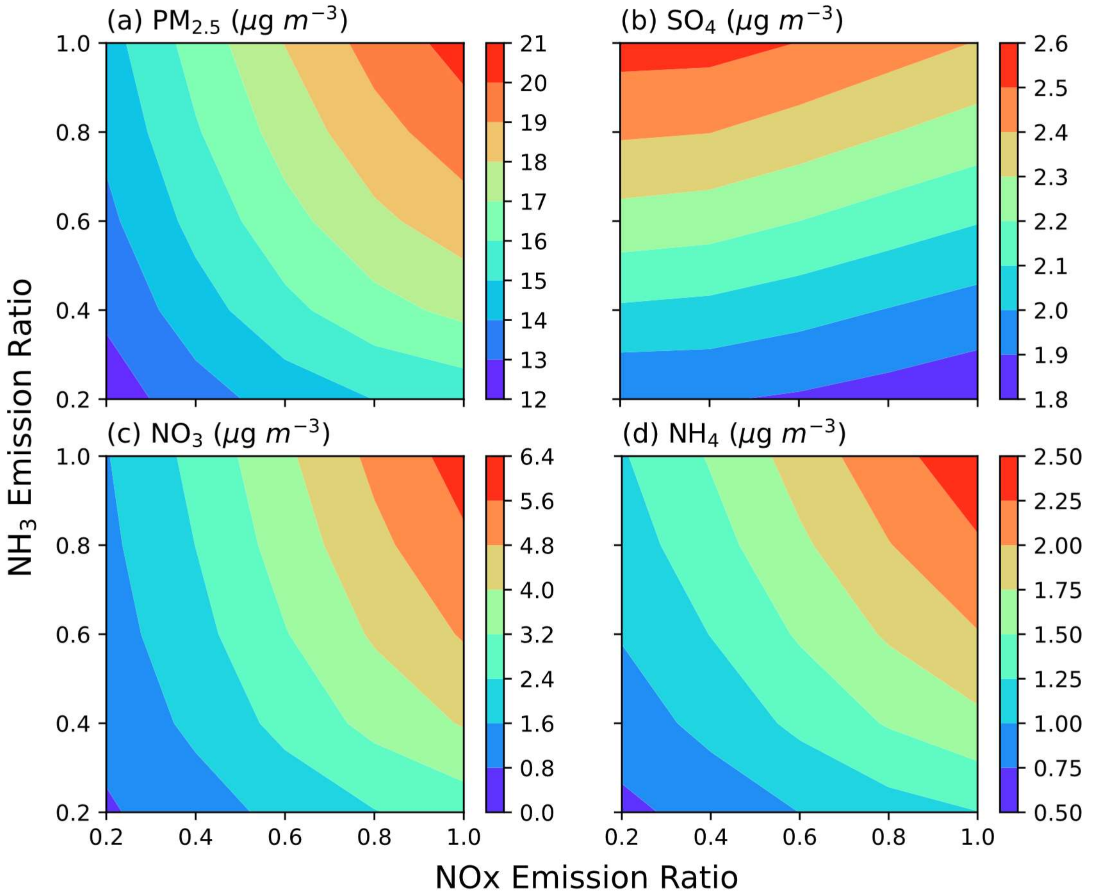

Figure S7: (a) $PM_{2.5}$, (b) sulfate, (c) nitrate, and (d) ammonium average concentration as a function of NOx (x-axis) and NH_3 (y-axis) emission ratios. Conditions: average data of central Taiwan from 1-14 December 2018 for the surface layer.

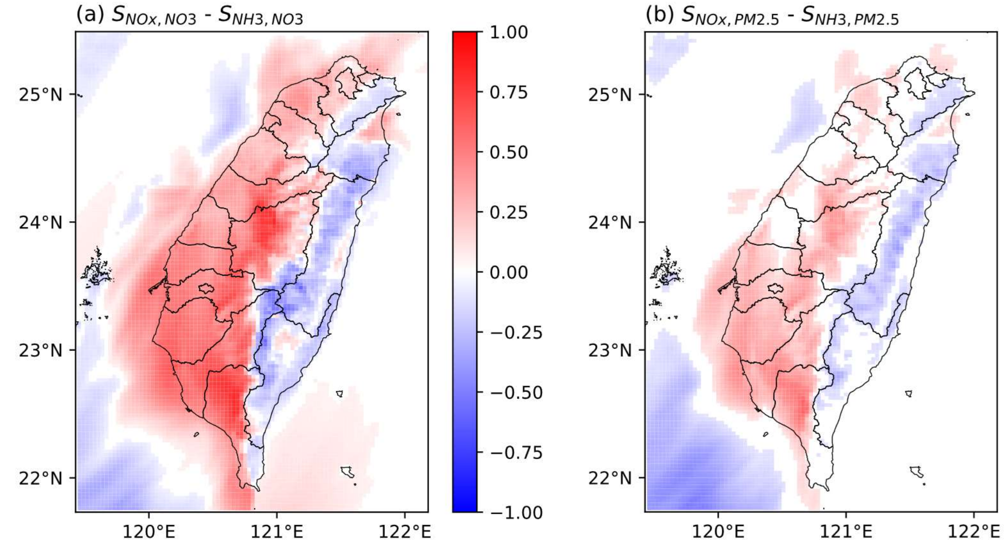

Figure S8: The difference of (a) nitrate and (b) $PM_{2.5}$ sensitivity coefficient map between NOx and NH_3 under the current condition (at NOx emission ratio of 0.9). Red regimes represent NOx-sensitive, blue regimes represent NH_3-sensitive, and white regimes represent neutral with values between -0.05 and 0.05. Conditions: average data from 1-31 December 2018 for the surface layer.

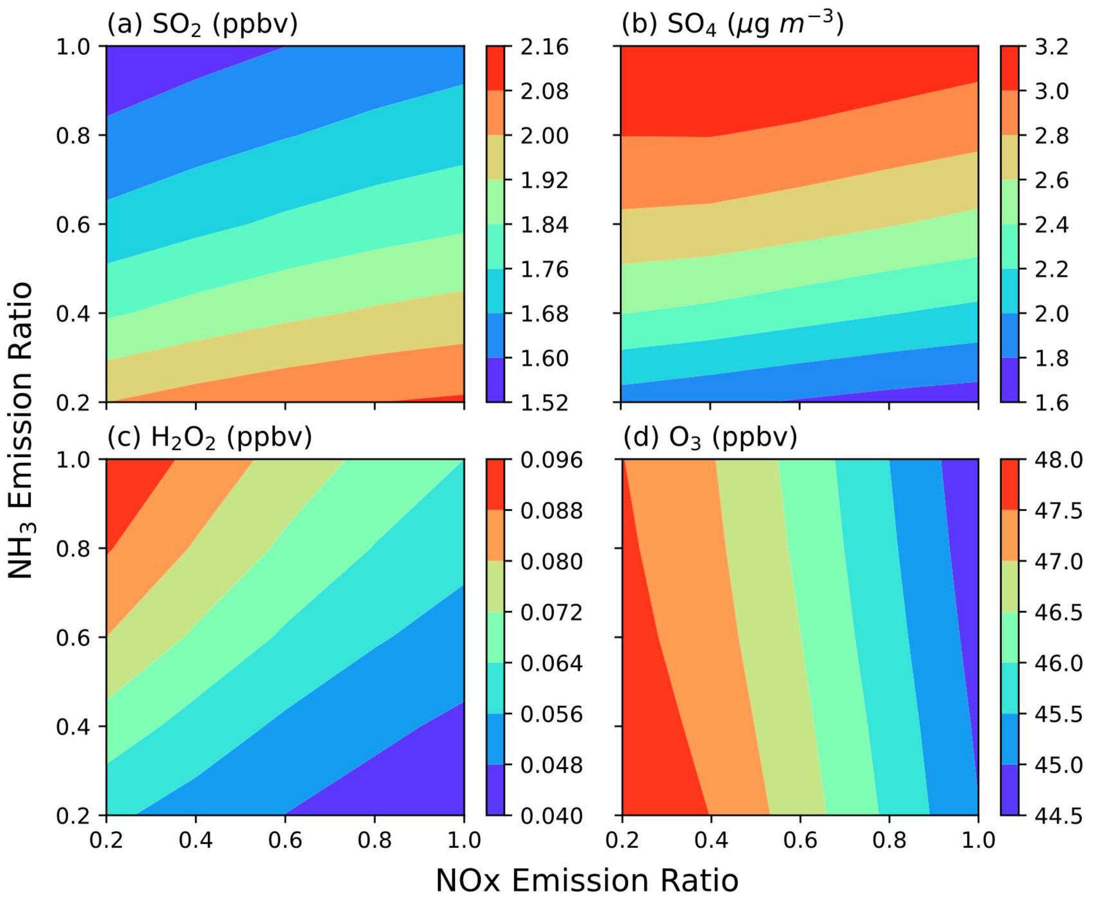

Figure S9: Average in-cloud (a) SO_2, (b) sulfate, (c) H_2O_2, and (d) ozone concentration as a function of NOx (x-axis) and NH_3 (y-axis) emission ratios. Conditions: average data of western Taiwan land regions in domain 4 from 1-14 December 2018 for the cloud grid points.

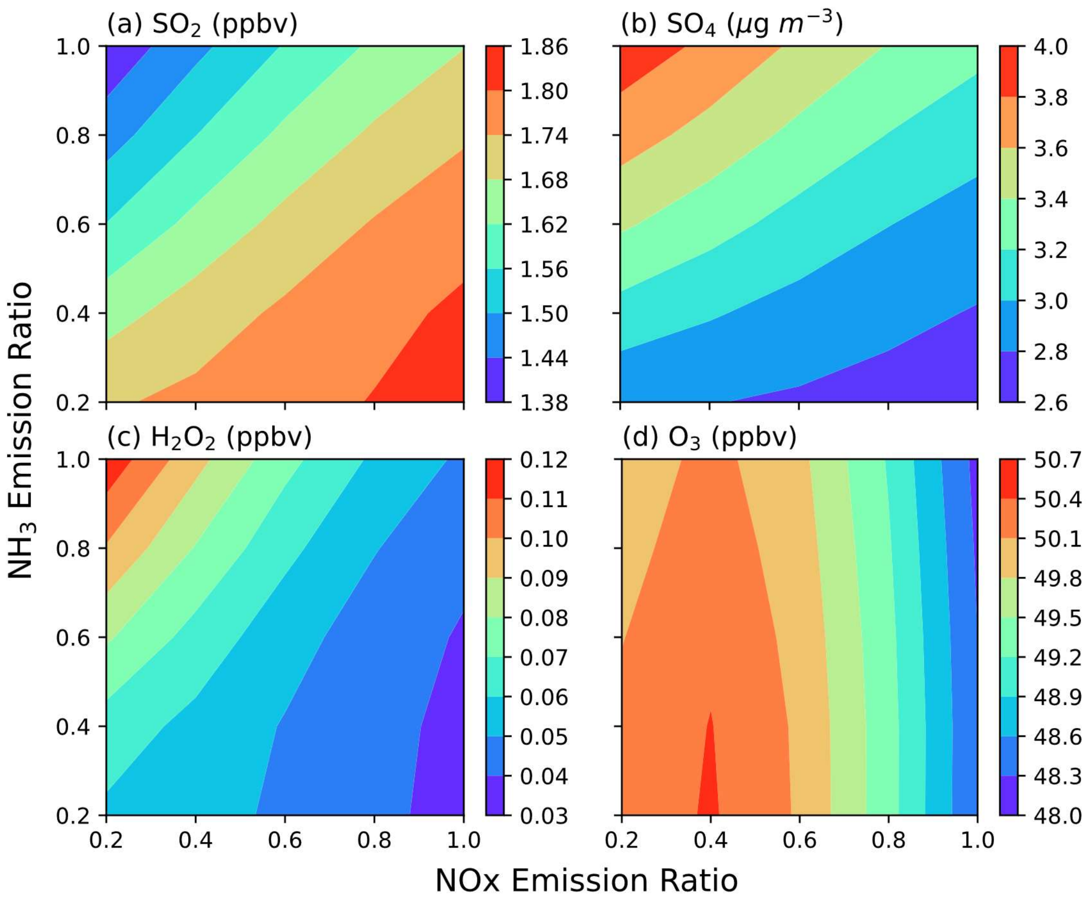

Figure S10: Average in-cloud (a) SO_2, (b) sulfate, (c) H_2O_2, and (d) ozone concentration as a function of NOx (x-axis) and NH_3 (y-axis) emission ratios. Conditions: average data of sea regions west of 121°E in domain 4 from 1-14 December 2018 for the cloud grid points.

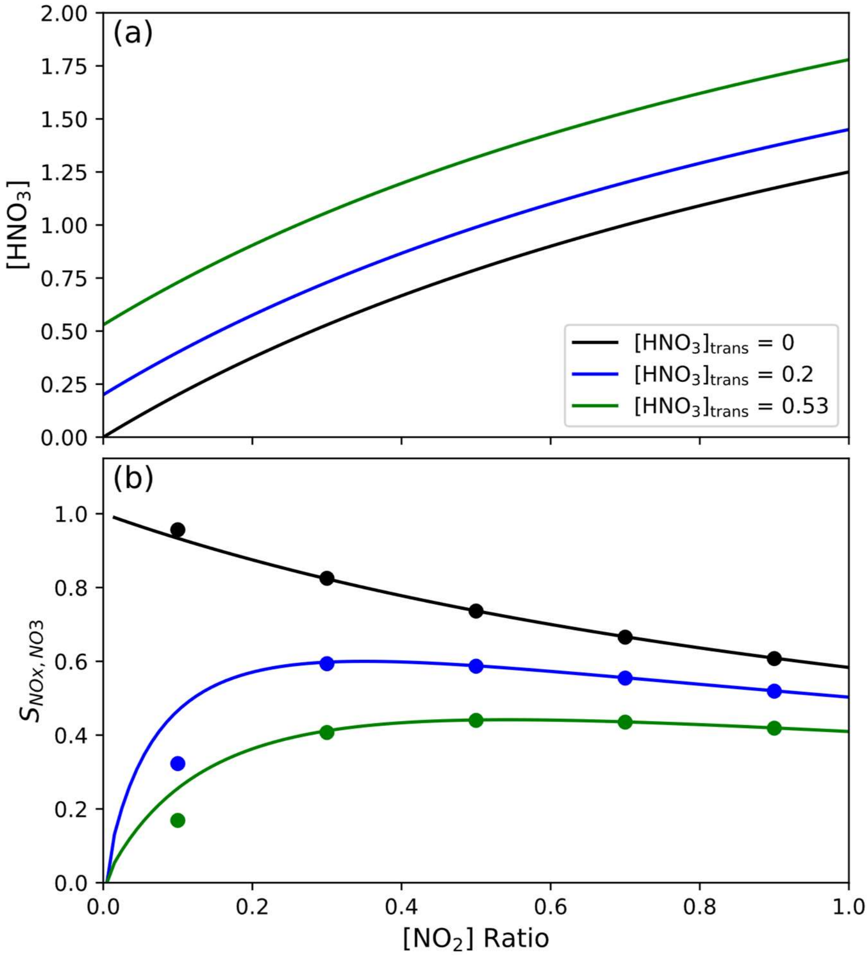

125

Figure S11: (a) HNO_3 concentration and (b) nitrate sensitivity coefficient of NOx (S_{NOx,NO_3}) as a function of NO_2 ratio.

Reference

Seinfeld, J. H., and Pandis, S. N.: Atmospheric Chemistry and Physics: From Air Pollution to Climate Change, Wiley, 2006.